Amlexanox reversibly inhibits cell migration and proliferation and induces desassembly of actin stress fibers in vitro

THE JOURNAL OF BIOLOGICAL CHEMISTRY
Vol. 275, No. 42, Issue of October 20, pp. 32753–32762, 2000

Printed in U.S.A.

Amlexanox Reversibly Inhibits Cell Migration and Proliferation and Induces the Src-dependent Disassembly of Actin Stress Fibers *in Vitro**

Received for publication, March 20, 2000, and in revised form, July 26, 2000
Published, JBC Papers in Press, July 31, 2000, DOI 10.1074/jbc.M002336200

Matteo Landriscina‡, Igor Prudovsky, Carla Mouta Carreira§, Raffaella Soldi, Francesca Tarantini¶, and Thomas Maciag‖

From the Center for Molecular Medicine, Maine Medical Center Research Institute, South Portland, Maine 04106

Amlexanox binds S100A13 and inhibits the release of fibroblast growth factor 1 (FGF1). Because members of the S100 gene family are known to be involved with the function of the cytoskeleton, we examined the ability of amlexanox to modify the cytoskeleton and report that amlexanox induces a dramatic reduction in the presence of actin stress fibers and the appearance of a random, non-oriented distribution of focal adhesion sites. Correspondingly, amlexanox induces the complete and reversible non-apoptotic inhibition of cell migration and proliferation, and although amlexanox does not induce either the down-regulation of F-actin levels or the depolymerization of actin filaments, it does induce the tyrosine phosphorylation of cortactin, a Src substrate known to regulate actin bundling. In addition, a dominant negative form of Src is able to partially rescue cells from the effect of amlexanox on both the actin cytoskeleton and cell migration. In contrast, the inhibition of cell proliferation by amlexanox correlates with the inhibition of cyclin D1 expression without interference of the receptor tyrosine kinase/mitogen-activated protein kinase signaling pathway. Last, the ability of amlexanox to inhibit FGF1 release is reversible and correlates with the restoration of the actin cytoskeleton, suggesting a role for the actin cytoskeleton in the FGF1 release pathway.

Amlexanox, an anti-allergic drug that binds S100A13, a relatively new member of the S100 gene family, is able to inhibit the heat shock-induced release of fibroblast growth factor (FGF1)[1] (1). FGF1 and FGF2 are the prototype members of a large family of heparin binding growth factor genes that regulate numerous biological processes, including mesoderm formation, neurogenesis, and angiogenesis *in vivo* (2). Since the FGF prototypes are characterized by the lack of a classical signal peptide sequence to provide access to the conventional endoplasmic reticulum-Golgi secretion pathway, it has been suggested that the release of both FGF1 and FGF2 may proceed through a novel release pathway (3). Our laboratory recently demonstrated that FGF1 is released as a reducing agent- and denaturant-sensitive complex, containing the p40 extravesicular domain of p65 Synaptotagmin (Syt) 1 *in vitro* (4, 5) and that FGF1, p40 Syt1, and S100A13 are components of a heparin binding complex *in vivo* (1).

It is well established that several members of the S100 gene family are associated with the cytoskeleton (6, 7) and that the actin cytoskeleton is essential in transmembrane signaling, endocytosis, and secretion (8). There is also increasing evidence that actin microfilaments and the subplasmalemmal cytoskeleton are involved in several aspects of vesicle transport (9). Indeed, in yeast, actin cytoskeleton mutants accumulate large secretory vesicles and exhibit defects in endocytosis that correlate with changes in actin-polarized organization (10). The actin cytoskeleton is also required by mammalian cells for cell proliferation, motility, and morphological changes (8).

The Src pathway also plays a central role in the modulation of the organization of the actin cytoskeleton in response to extracellular stimuli through the phosphorylation of several actin-binding proteins including cortactin (11, 12). Indeed, the activation of the Src pathway correlates with the induction of cell migration and the redistribution of cortactin and F-actin, in response to FGF1 (13).

Since (i) amlexanox is an inhibitor of FGF1 and p40 Syt1 release *in vitro* (1), (ii) this reagent binds S100A13, a member of the heparin binding complex containing p40 Syt1 and FGF1 (1, 14), and (iii) members of the S100 gene family are involved in the regulation of cytoskeletal function (6, 7), we examined the effect of amlexanox on cell morphology, migration, proliferation, and cytoskeletal organization. We report that amlexanox induces a Src-dependent phosphorylation of cortactin that may be responsible for the reversible inhibition of cell migration and organization of actin stress fibers and induces a Src-independent reversible inhibition of cell proliferation that correlates with cyclin D1 down-regulation.

MATERIALS AND METHODS

Cell Culture—Human umbilical vein endothelial cell (HUVEC), NIH 3T3, Swiss 3T3, and L6 cells were grown as described previously (13, 15). Newborn rat aorta smooth muscle cells were grown in a 1:1 mixture of DMEM (Cellgro) and Ham's F-12 (Cellgro) supplemented with 5% (v/v) fetal bovine serum (Hyclone) (16) and human fibroblasts (IMR 90 strain; ATCC) were grown in DMEM supplemented with 10% (v/v) fetal bovine serum. Glioma cell lines, U-251Mg and U-563Mg, a gift of B.

* This work was supported in part by National Institutes of Health Grants HL35627, HL32348, and AG07450 (to T. M.). The costs of publication of this article were defrayed in part by the payment of page charges. This article must therefore be hereby marked "*advertisement*" in accordance with 18 U.S.C. Section 1734 solely to indicate this fact.
‡ Supported by a fellowship from the Catholic University of Rome.
§ Present address: Massachusetts General Hospital, Harvard Medical School, 100 Blossom St., Boston, MA 02114.
¶Present address: Dept. of Geriatric Medicine, University of Florence, School of Medicine, Florence, Italy.
‖ To whom correspondence should be addressed: Center for Molecular Medicine, Maine Medical Center Research Institute, 125 John Roberts Rd., South Portland, Maine 04106. Tel.: 207-761-9783; Fax: 207-828-8071; E-mail: maciat@mail.mmc.org.
[1] The abbreviations used are: FGF, fibroblast growth factor; BCS, bovine calf serum; DMI, defined medium with insulin; dn, dominant negative; FAK, focal adhesion kinase; Syt, synaptotagmin; NBD, 12-(*N*-methyl-*N*-(7-nitrobenz-2-oxa-1,3-diazol-4-yl)); HUVEC, human umbilical vein endothelial cells; DMEM, Dulbecco's modified Eagle's medium; Pipes, 1,4-piperazinediethanesulfonic acid; ERK, extracellular signal-regulated kinase; PDGF, platelet-derived growth factor; PDGFR, PDGF receptor; PAGE, polyacrylamide gel electrophoresis.

Westermark (University of Uppsala, Uppsala, Sweden), were grown in DMEM supplemented with 10% (v/v) bovine calf serum (BCS; Hyclone) (17). NIH 3T3 cells were transfected with a mutated form of *Xenopus laevis* Src in which lysine 294 was replaced by alanine and tyrosine 526 was replaced by phenylalanine (18). The Src mutant, kindly provided by R. Friesel was cloned into pcDNA 3.1/Hygro vector (Invitrogen) using the *Xho*I and *Xba*I restriction sites. The transfection was performed using a multi-component lipid-based reagent (FuGENE 6, Roche Molecular Biochemicals). Swiss 3T3 or NIH 3T3 cells were made quiescent by incubating the confluent monolayer in serum-free hormone-defined medium (DMI) as described (19). Amlexanox (AA673) was a generous gift of Takeda Chemical Industries, Osaka, Japan and was solubilized in equimolar NaOH. Latrunculin and jasplakinolide were purchased from Biomol and Molecular Probes, respectively.

Fluorescence Microscopy and F-actin Expression—Immunofluorescence and F-actin staining were performed as described previously (13) Focal adhesion sites, vinculin and tubulin, were stained using, respectively, a monoclonal anti-phosphotyrosine (Upstate Biotechnology), a monoclonal anti-vinculin (Sigma), and a monoclonal anti-tubulin (Sigma) antibody. To examine F-actin expression, cells were fixed in 4% (v/v) formaldehyde in buffer A (5 mM Pipes, pH 7.2, containing 5 mM KCl, 138 mM NaCl, 4 mM $NaHCO_3$, 0.4 mM KH_2PO_4, 2 mM $MgCl_2$, and 2 mM EGTA) and permeabilized with 0.5% (v/v) Triton X-100 in buffer A for 20 min. The monolayers were rinsed in 0.1 M glycine in buffer A for 10 min and washed 5 times with buffer A. The cells were incubated in 1 μM NBD-phallacidin (Molecular Probes) in buffer A for 1 h and washed 5 times for 5 min with buffer A, and the F-actin-bound NBD-phallacidin was extracted with methanol at 4 °C for 90 min. Simultaneously, cells plated at the same density and treated as described above were used to quantitate cell number using a hematocytometer. Fluorescence of the methanol extraction solution was measured at 465-nm excitation and 535-nm emission and normalized against cell number (21).

Immunoprecipitation and Immunoblot Analysis—Cells were grown to confluence and incubated for 48 h in DMI, washed with cold phosphate-buffered saline, scraped in cold phosphate-buffered saline containing 1 mM sodium orthovanadate, and collected by centrifugation ($1.000 \times g$, 10 min). Cell pellets were lysed for 20 min in 0.5 ml of cold lysis buffer (20 mM Tris, pH 7.5, containing 300 mM sucrose, 60 mM KCl, 15 mM NaCl, 5% (v/v) glycerol, 2 mM EDTA, 1% (v/v) Triton X-100, 1 mM phenylmethylsulfonyl fluoride, 2 μg/ml aprotinin, 2 μg/ml leupeptin, and 0.2% (w/v) deoxycholate) containing 1 mM sodium orthovanadate, and cell lysates were clarified by centrifugation ($2.000 \times g$, 10 min). For actin immunoblot analysis, cells were treated as described above except the cells were not pretreated with DMI and were lysed in cold lysis buffer not containing sodium orthovanadate. Actin levels were evaluated using an anti-actin monoclonal antibody from Sigma. For cyclin D1 analysis, quiescent Swiss 3T3 cells were treated for 6 h with either 1 mM amlexanox or with 10 ng/ml FGF1 or with both and lysed as described above. Protein concentration was determined using the Pierce BCA protein assay kit. To examine protein tyrosine phosphorylation, immunoprecipitation was performed using a rabbit antibody against cortactin (12), a rabbit antibody against focal adhesion kinase (Sigma), two rabbit antibodies against ERK1 and ERK2 (Santa Cruz), a rabbit antibody against PDGFR type B (Upstate Biotechnology), a rabbit antibody against FGFR1 (13), and a rabbit antibody against the insulin receptor β subunit (Upstate Biotechnology) as described previously (12).

Analysis of Cell Migration, Cell Proliferation, and Apoptosis—Cell proliferation was assessed as described previously (15), and cell migration was evaluated using an *in vitro* model of wound repair as described (22). To examine apoptosis, confluent monolayers of HUVEC and NIH 3T3 cells were incubated with or without 0.375 M or 1 mM amlexanox. To prevent the loss of floating apoptotic cells from the cell population, fresh medium was added every 2 days to the culture dish without removing the old medium. After 3 days, the cells were harvested by trypsin digestion, and the floating cells were independently collected by centrifugation and combined with the cells obtained from the monolayer. The cells were washed with phosphate-buffered saline, and smears were prepared and fixed in 70% (v/v) ethanol. The cells were stained with 100 ng/ml Hoechst #33258 (Sigma) for 1 min, and apoptotic nuclei with fragmented chromatin were quantitated using a fluorescence microscope. Five hundred cells were counted per treatment, and apoptotic cells were expressed as a percentage of total cells counted. The experiment was repeated in triplicate using two wells for each condition.

Analysis of FGF1 Release—The reversibility of FGF1 release after amlexanox pretreatment was performed using NIH 3T3 cells stably transfected with FGF1 (23). Cells were grown until 70% confluence and incubated overnight in the presence or absence of 1 mM amlexanox. The monolayers were washed with DMEM containing 5 units/ml heparin (The Upjohn Co.). Cells previously treated with amlexanox were also incubated in DMEM containing 5 units/ml heparin but in the presence or absence of 0.375 mM amlexanox, and the cells, previously not treated with amlexanox, were further incubated under amlexanox-free conditions. The cell populations were subjected to heat shock (42 °C for 110 min) as previously reported (5, 23). To evaluate the effect of latrunculin on FGF1 and p40 Syt1 release, NIH 3T3 cells transfected with FGF1 and p65 Syt1 were grown until 70% confluent and were subjected to heat shock (42 °C, 110 min) in the presence and absence of 400 nM latrunculin (Biomol). Media conditioned by this response were processed and analyzed by FGF1 and/or Syt1 immunoblot analysis as described previously (5, 23).

RESULTS

Amlexanox Reversibly Modifies Cell Morphology—We have previously demonstrated that the S100A13 binding compound, amlexanox, inhibits the release of FGF1 and p40 Syt1 from NIH 3T3 cells in response to heat shock (1). Since several members of the S100A13 family are cytoskeleton-associated proteins (6, 7), we questioned whether amlexanox could modify cell morphology. After exposure for 24 h to amlexanox, NIH 3T3 cells exhibited a dramatic change in their morphology that included a larger and more flattened phenotype and often displayed long processes that are stable for at least 10 days (Fig. 1, *A* and *B*). Interestingly, the amlexanox-induced morphology of NIH 3T3 cells completely reverted to the normal phenotype 2 days after the removal of amlexanox.

Amlexanox was also able to produce similar, reversible effects on cell morphology in a large variety of cell lines, including HUVEC (Fig. 1, *C* and *D*), Swiss 3T3 cells, human IMR90 fibroblasts, newborn rat aorta smooth muscle cells, rat L6 myoblasts, and the murine glioma cell lines U251Mg and U563Mg (data not shown). Interestingly, the phenotype exhibited by HUVEC populations resembled the phase contrast morphology of the senescent HUVEC phenotype resulting from extended serial propagation *in vitro* (24). In addition, serum starvation accelerated the effects of amlexanox upon cell morphology. NIH and Swiss 3T3 cells serum-starved for 2 days and then treated with 1 mM amlexanox exhibited a more dramatic and rapid morphological change than cells maintained in complete cell culture medium (data not shown).

Amlexanox Induces Changes in the Actin Cytoskeleton—The induction and reversion of morphological changes produced by amlexanox prompted us to examine the organization of the cytoskeleton using HUVEC populations which are quite sensitive to agents that promote apoptosis. Interestingly, we observed no differences in the level of apoptosis between control (2.5% ± 1.0) and amlexanox-treated (2.6% ± 1.1) HUVEC populations as well as NIH and Swiss 3T3 cells (data not shown), using an assessment of chromatin fragmentation by Hoechst staining. In addition, fluorescein isothiocyanate-phalloidin staining of HUVEC populations treated for 4 days with amlexanox revealed a dramatic attenuation of the F-actin cytoskeleton (Fig. 1, *E* and *F*). Indeed, the amlexanox-treated cells exhibited either a complete absence or strong down-regulation of phalloidin-positive F-actin stress fibers. However, the subplasmalemmal F-actin cortex remained readily apparent in the amlexanox-treated cells. This change in the appearance of the F-actin cytoskeleton became visible as early as 4 to 8 h after the addition of amlexanox and was fully prominent after 24 h (data not shown). Similar changes in the F-actin cytoskeleton were induced by 1 mM amlexanox in Swiss (data not shown) and NIH 3T3 cells (Fig. 3, *A* and *B*). In addition, the changes in the F-actin cytoskeleton induced by amlexanox were reversible. Indeed, 2 hours after the removal of amlexanox, the majority of the HUVEC population previously treated for 4 days with amlexanox exhibited the presence of prominent F-actin stress fibers *in vitro* (Fig. 1*G*). In contrast, however, despite the dra-

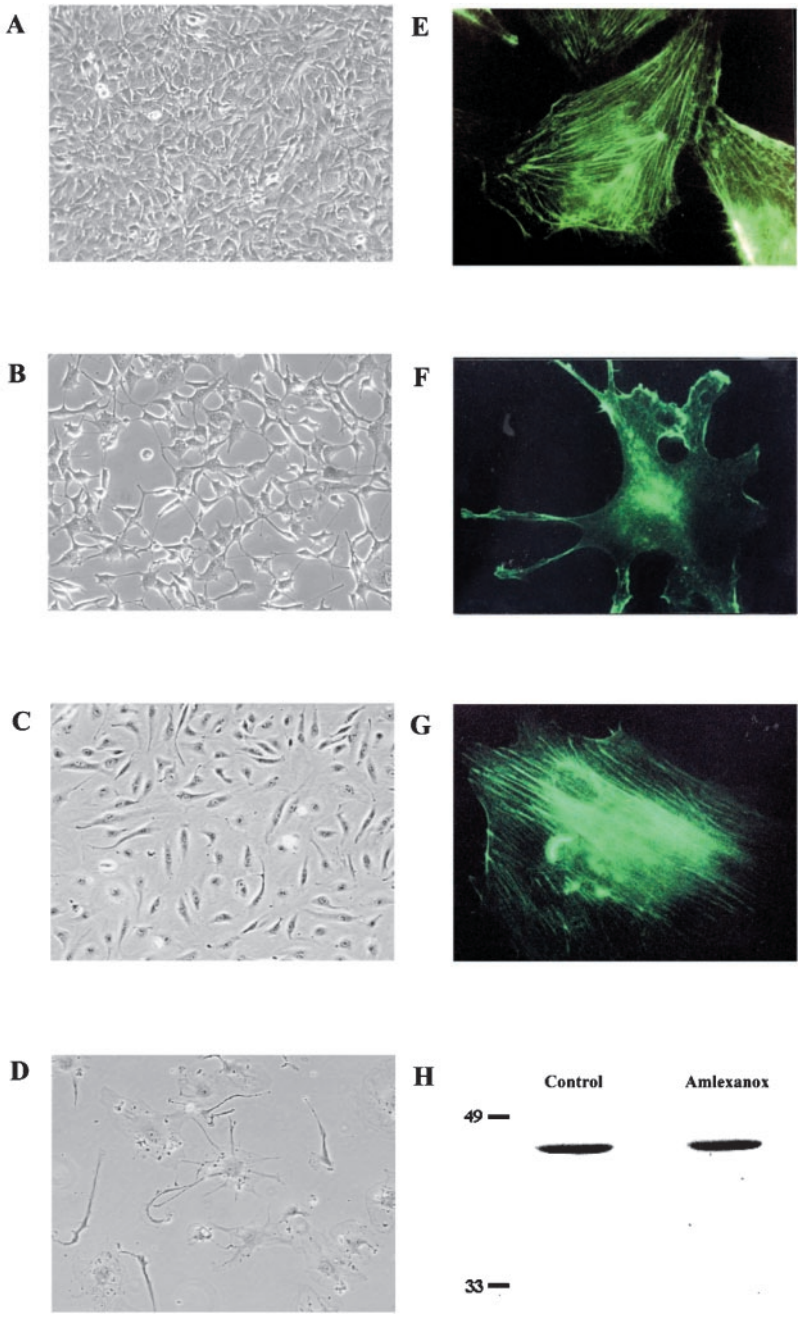

FIG. 1. **The effect of amlexanox on cell morphology and changes in the appearance of the actin cytoskeleton.** NIH 3T3 cells (*A* and *B*) and HUVEC (*C* and *D*) were grown for 4 days as described under "Materials and Methods" in the absence (*A* and *C*) or in the presence of 1 mM (*B*) or 0.375 mM (*D*) amlexanox. Phase contrast microscopy (*A–C*, 10×; *D*, 20×) was used to record the phenotype. Fluorescence microscopy of actin distribution (*E–G*) is shown in HUVEC populations incubated in the presence (*F*) or in the absence (*E*) of 0.375 mM amlexanox for 4 days. Actin distribution in HUVEC populations treated with 0.375 mM amlexanox for 4 days and further incubated for 2 h in normal growth medium without amlexanox (*G*) is shown. Fluorescent photomicrographs were taken with a 100× objective. *H*, immunoblot analysis of total actin levels in HUVEC populations exposed for 2 days in the presence or absence of 0.375 mM amlexanox.

matic attenuation of the F-actin cytoskeleton, the amlexanox-treated HUVEC population did not exhibit any significant change in the organization of their tubulin-containing microtubule and vimentin-containing intermediate filament networks (data not shown). Fluorescein isothiocyanate-phalloidin staining of amlexanox-treated, serum-deprived NIH and Swiss 3T3 cells exhibited a very rapid (30 min to 1 h) disappearance of actin stress fibers and the fragmentation of the actin cytoskeleton (data not shown).

The strong attenuation of F-actin stress fibers after treatment with amlexanox prompted us to evaluate the total level of actin and the level of F-actin in HUVEC populations before and after exposure to amlexanox for 48 h. As shown in Fig. 1*H*, actin immunoblot analysis revealed no difference in the levels of actin expression between amlexanox-treated and control HUVEC populations. Similarly, we did not observe a difference in the content of polymerized actin as measured by the fluorescence of methanol-extracted NBD phallacidin between the control (0.045 ± 0.003 relative units/cell) and amlexanox-treated (0.056 ± 0.004 relative units/cell) HUVEC populations. The presence of 1 mM amlexanox did not alter the steady state levels of the actin transcript in Swiss 3T3 cells as assessed by reverse transcriptase-polymerase chain reaction (data not shown). In addition, jasplakinolide, an agent that binds and stabilizes filamentous actin (20), prevented the amlexanox-induced changes in cell morphology and attenuation of F-actin stress fibers (data not shown).

Amlexanox Induces Cortactin Tyrosine Phosphorylation—Because (i) amlexanox was able to affect the organization of actin stress fibers without affecting the expression of actin and its polymerization and (ii) serum deprivation potentiated the effect of amlexanox, we evaluated the level of tyrosine phosphorylation of cortactin, an actin-binding protein whose phosphorylation by Src has been implicated in the rearrangement of the actin cytoskeleton after growth factor stimulation (25). Since Swiss 3T3 cells under conditions of serum deprivation

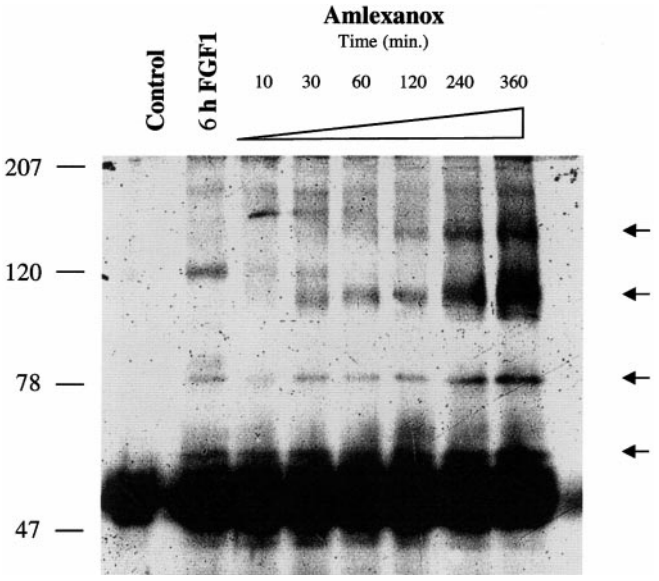

FIG. 2. **Tyrosine phosphorylation of cortactin in Swiss 3T3 cells treated with amlexanox.** Swiss 3T3 cells were grown to confluence and incubated for 48 h in DMI. Quiescent cells were further incubated with either 1 mM amlexanox for the times indicated or with 10 ng/ml FGF1 for 6 h. Cell lysates were immunoprecipitated with rabbit anti-cortactin antibody 2719 (12), resolved by 8% (w/v) acrylamide SDS-PAGE, and subjected to immunoblot analysis with an antiphosphotyrosine antibody (Upstate Biotechnology) as described under "Materials and Methods." The *arrows* indicate the position of cortactin and three other phosphotyrosine-containing proteins with approximate masses of 60, 110, and 140 kDa.

display a very low level of cortactin tyrosine phosphorylation, we examined this cell culture system for the tyrosine phosphorylation of cortactin in response to amlexanox. As shown in Fig. 2, we observed that the amlexanox was able to stimulate the tyrosine phosphorylation of cortactin in a rapid and sustained manner. Interestingly, the intensity of cortactin tyrosine phosphorylation stimulated by amlexanox (Fig. 2) appeared to be greater than that achieved by FGF1 after a 6-h incubation period. Phosphotyrosine analysis of cortactin immunoprecipitates also revealed the presence of other tyrosine-phosphorylated proteins including a p60 protein that was phosphorylated in parallel with cortactin in amlexanox-treated cells as well as in cells stimulated with FGF1 for 6 h (Fig. 2). Two additional proteins, p110 and p140, were also phosphorylated on tyrosine residues in an amlexanox-dependent manner 30 min and 2 h after amlexanox treatment but not in the presence of FGF1 (Fig. 2).

A Dominant Negative Form of Src Prevents the Amlexanox-induced Collapse of Actin Cytoskeleton and Down-regulates Cortactin Tyrosine Phosphorylation in Amlexanox-treated Cells—Since (i) cortactin is a protein phosphorylated by Src in response to extracellular growth factors stimulation (12), (ii) phosphotyrosine analysis of cortactin immunoprecipitates after amlexanox treatment revealed the presence of a p60 protein (Fig. 2), and (iii) cortactin is involved in the regulation of actin bundling (25), we investigated the involvement of the Src phosphorylation in the amlexanox-dependent collapse of the actin cytoskeleton using a dominant negative (dn) mutant of Src (18). Stable dnSrc NIH 3T3 cell transfectants were obtained, and these displayed enhanced levels of the Src transcript and protein, as determined by reverse transcriptase-polymerase chain reaction and immunoblot analysis, respectively (data not shown). Interestingly, treatment with 1 mM amlexanox for 48 h in the presence of 10% (w/v) BCS resulted in the disappearance of actin stress fibers in NIH 3T3 cells (Fig. 3, *A* and *B*) but failed to completely destroy stress fibers in dnSrc NIH 3T3 cell transfectants (Fig. 3, *C* and *D*). Correspondingly, amlexanox also induced a less dramatic morphological change in dnSrc NIH 3T3 cell transfectants (data not shown).

Although NIH 3T3 cells displayed high levels of cortactin tyrosine phosphorylation under conditions of cellular quiescence and these levels were not significantly altered by the addition of either amlexanox or FGF1, cortactin tyrosine phosphorylation was significantly reduced in the dnSrc NIH 3T3 cell transfectants treated for 6 h with 1 mM amlexanox (Fig. 4*A*). This decrease in cortactin tyrosine phosphorylation also correlated with the conservation of the actin cytoskeleton observed in the amlexanox-treated dnSrc NIH 3T3 cell transfectants (Fig. 3).

Amlexanox Reversibly Inhibits Cell Migration—Since (i) amlexanox modifies the reorganization of the actin cytoskeleton through a Src-related mechanism and (ii) Src is involved in the regulation of cell migration (13), we examined the ability of amlexanox to interfere with cell motility (22). Indeed, the migratory ability of NIH 3T3 cells was significantly diminished by the presence of amlexanox in a dose-dependent manner, with a half-maximum value of approximately 100 μM amlexanox (Fig. 5*A*). The vehicle (1 mM NaOH) used to deliver amlexanox did not modify the migratory ability of NIH 3T3 cell population (Fig. 5*A*). Similar results were obtained using Swiss 3T3 cells and HUVEC (data not shown). This repression of cell migration was reversible (data not shown) and occurred at concentrations of amlexanox similar to those that were able to alter both cell morphology and actin cytoskeleton.

Since dnSrc NIH 3T3 cell transfectants exhibited an attenuation of the effect of amlexanox on the actin cytoskeleton, we evaluated the capacity of amlexanox to suppress the motility of these cells. As shown in Fig. 5*B*, amlexanox exhibited a strong inhibition of NIH 3T3 cell migration, whereas the inhibition of cell motility was less dramatic in two clones of the dnSrc NIH 3T3 cell transfectants treated with amlexanox.

Amlexanox Induces Changes in Focal Adhesion Site Distribution and Modifies the Tyrosine Phosphorylation of Focal Adhesion Kinase—Since actin stress fibers are known to be structurally linked to focal adhesion sites through α-actinin (26) and are involved in the regulation of cell migration and adhesion (27), we questioned whether amlexanox treatment was able to modify the organization of focal adhesion sites in NIH 3T3 cells and dnSrc NIH 3T3 cell transfectants. Immunohistochemical staining for vinculin, a component of focal adhesion sites (28), demonstrated that amlexanox treatment in the presence of serum resulted in a significant decrease in the intensity and the redistribution of focal adhesion sites in NIH 3T3 cells. Instead of the parallel and well oriented focal adhesion sites that are often concentrated at the leading edge of the cell and usually observed in cells undergoing migration (24), we observed a radial or random distribution of the vinculin-positive focal adhesion sites in the amlexanox-treated cells (Fig. 3, *E* and *F*). This phenotype is usually associated with non-migratory and "sedentary" populations of cells (24). The effect of amlexanox on focal adhesion site orientation in the dnSrc NIH 3T3 transfectants was not as dramatic as that observed with control NIH 3T3 cells (Fig. 3, *G* and *H*), and this is consistent with the resistance of dnSrc NIH 3T3 cell transfectants to amlexanox-induced inhibition of cell migration. In addition, under short term conditions of serum deprivation, amlexanox produced a more dramatic and faster disappearance of focal adhesion sites in NIH 3T3 cells, whereas amlexanox treatment produced only a partial redistribution of focal adhesion sites in the dnSrc NIH 3T3 transfectants (data not shown).

Since Src has been demonstrated to regulate cell migration by forming a complex with focal adhesion kinase (FAK) in focal

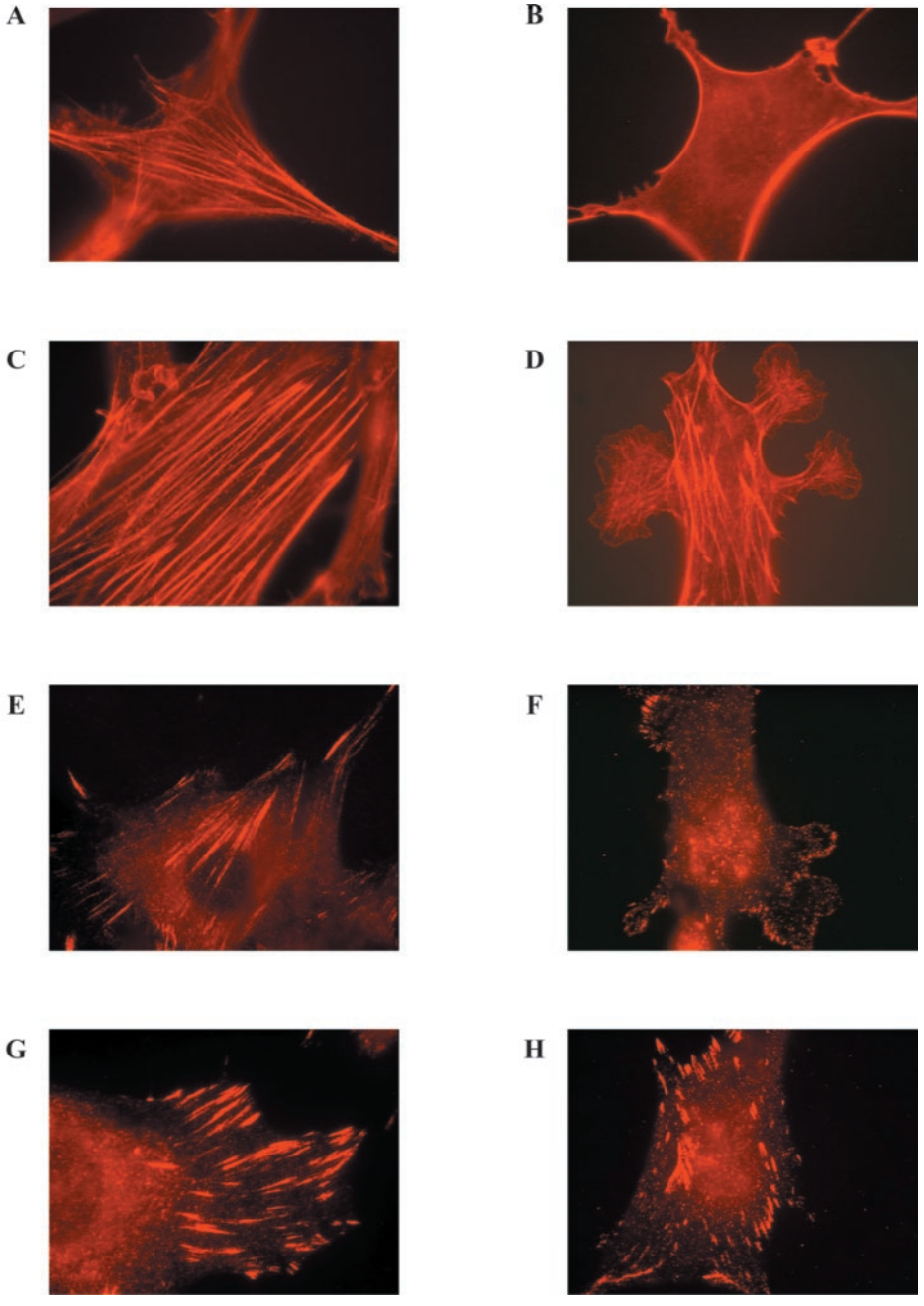

FIG. 3. **Changes in the actin cytoskeleton and immunofluorescence microscopy of focal adhesion sites in NIH 3T3 and dnSrc NIH 3T3 cells transfectants treated with amlexanox.** Fluorescence microscopy is shown of actin distribution in NIH 3T3 (*A* and *B*) and dnSrc NIH 3T3 cell transfectants (*C* and *D*) incubated in the presence (*B* and *D*) and absence (*A* and *C*) of 1 mM amlexanox for 2 days. Immunofluorescent microscopy of focal adhesion sites is shown in NIH 3T3 (*E* and *F*) and dnSrc NIH 3T3 cell transfectants (*G* and *H*) incubated in the presence (*F* and *H*) or absence (*E* and *G*) of 1 mM amlexanox for 2 days. Fluorescent photomicrographs were taken with a 100× objective.

adhesion sites (29), we examined whether the amlexanox-induced redistribution of focal adhesion sites in NIH 3T3 cells correlated with a change in the tyrosine phosphorylation of FAK. Phosphotyrosine analysis of FAK immunoprecipitates exhibited similar levels of tyrosine phosphorylation in control NIH 3T3 and dnSrc NIH 3T3 cell transfectants (Fig. 4*B*). After treatment with 1 mM amlexanox for 6 h under serum-free conditions, cells displayed a moderate down-regulation of FAK phosphorylation in both control NIH 3T3 and dnSrc NIH 3T3 cell transfectants (Fig. 4*B*). This was also observed in Swiss 3T3 cells (data not shown).

Amlexanox Reversibly Inhibits Cell Proliferation—Since (i) amlexanox inhibits the release of FGF1 from NIH 3T3 cells in response to heat shock (1), (ii) the ability of FGF1 to induce biologic responses requires its presence in the extracellular compartment to mediate receptor-dependent signaling (2, 3), and (iii) other reagents that affect the integrity of actin cytoskeleton also inhibit cell proliferation (30), we examined the ability of amlexanox to modify *in vitro* the growth of HUVEC, cells that are dependent upon the presence of a source of extracellular FGF for growth (15). Amlexanox was able to inhibit the growth of HUVEC (Fig. 6*A*) in a dose-dependent manner, with a half-maximum value of approximately 30 μM amlexanox (data not shown). The vehicle (0.375 mM NaOH) used to deliver amlexanox did not modify the proliferative ability of the HUVEC population (Fig. 6*A*). The ability of amlexanox to repress HUVEC growth was time-dependent, with significant inhibition of HUVEC growth observed after 72 h of treatment with the drug (data not shown). We also examined the ability of amlexanox to inhibit DNA synthesis. HUVEC populations were treated for 2 or 4 days with amlexanox in a concentration-dependent manner, and their ability to incorporate [^{3}H]thymidine in the nucleus was assessed by autoradiography. We observed a dose-dependent inhibition of DNA synthesis in cells treated with amlexanox with a half-maximal effect at 30 μM amlexanox (data not shown). Similar results were observed with human IMR90 fibroblasts, newborn rat aorta smooth muscle cells, rat L6 myoblasts, NIH 3T3 cells,

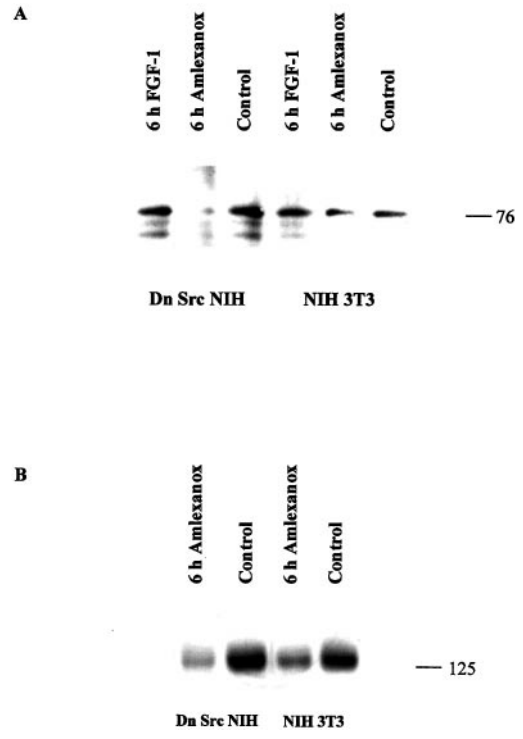

FIG. 4. **Tyrosine phosphorylation of cortactin and FAK in NIH 3T3 and dnSrc NIH 3T3 cell transfectants treated with amlexanox.** *A*, cortactin phosphotyrosine analysis. DnSrc NIH 3T3 cell transfectants were grown to confluence and incubated for 48 h in DMI. Quiescent cells were further incubated in DMI for 6 h or were incubated for 6 h in DMI containing 1 mM amlexanox or 10 ng/ml FGF1. Cortactin immunoprecipitation and immunoblot were performed as described under "Materials and Methods." *B*, FAK phosphotyrosine analysis. Quiescent NIH 3T3 and dnSrc NIH 3T3 cell transfectants were incubated in DMI or in DMI containing 1 mM amlexanox for 6 h. Cell lysates were immunoprecipitated with a rabbit anti-FAK antibody, resolved by 7.5% (w/v) acrylamide SDS-PAGE, and subjected to immunoblot analysis with an antiphosphotyrosine antibody as described under "Materials and Methods."

Swiss 3T3 cells, and the murine glioma cell lines U251Mg and U563Mg. Although the Swiss 3T3 and NIH 3T3 cells were less responsive to amlexanox with half-maximal inhibition of cell growth at 300 μM, the remainder of the cells exhibited growth inhibition at concentrations of amlexanox similar to that observed with HUVEC populations (data not shown).

We also examined whether the inhibition of cell growth was reversible. Confluent populations of HUVEC were exposed to 0.375 mM amlexanox, and after 4 days, the cells were harvested by trypsin digestion and replated, and the amlexanox-pretreated cells were incubated with or without 0.375 mM amlexanox. As shown in Fig. 6*A*, the HUVEC population previously exposed to amlexanox initially exhibited a decrease in their proliferative ability but after 3 days exhibited a population doubling time similar to the control, amlexanox-free population. In contrast, the HUVEC population previously exposed to amlexanox was not able to proliferate if amlexanox remained present in the cell culture medium (Fig. 6*A*). Flow cytometry analysis of HUVEC treated with amlexanox and Swiss 3T3 cells synchronized by incubation in the presence of either DMI and/or 4 mM thymidine and stimulated with serum in the presence and absence of amlexanox demonstrated that amlexanox inhibits the cell cycle in G_1 and G_2 phases (data not shown).

Amlexanox Down-regulates Cyclin D1 Expression without Affecting the FGF Receptor Signaling—Because amlexanox was able to reversibly inhibit the cell proliferation blocking cell cycle in both G_1 and G_2 phases, we evaluated the expression of cyclin D1, a protein that plays a key role in the progression from G_0 through G_1 into the S phase and is up-regulated in G_1 phase of cell cycle (24). As shown in Fig. 6*C*, quiescent Swiss 3T3 cells did not express detectable levels of cyclin D1, and amlexanox was not able to induce cyclin D1 expression. However, cells stimulated for 6 h with FGF-1 demonstrated an induction of cyclin D1 protein expression, and this induction was inhibited by the simultaneous exposure of cells to 1 mM amlexanox (Fig. 6*C*). We also evaluated cyclin D1 protein levels during Swiss 3T3 cell proliferation in response to serum in the presence and absence of 1 mM amlexanox. As shown in Fig. 6*C*, proliferating populations of Swiss 3T3 cells exhibited high levels of cyclin D1, but after exposure to amlexanox, the levels of cyclin D1 were significantly and rapidly decreased.

To understand if the amlexanox-dependent inhibition of cyclin D1 induction was the result of its ability to interfere with polypeptide growth factor/receptor/Ras/mitogen-activated protein kinase signaling pathways, we evaluated the capacity of FGF1, PDGF-BB, and insulin to activate their receptors in the presence of amlexanox. Quiescent Swiss 3T3 cells were treated for 6 h with 1 mM amlexanox or incubated for an additional 6 h in serum-free medium without amlexanox and then were stimulated for 30 min with either 10 ng/ml FGF1, 5 ng/ml PDGF-BB, or 1 μg/ml insulin in the presence or absence of amlexanox. Phosphotyrosine immunoblot analysis following FGFR-1, PDGFR type B, and insulin receptor β subunit immunoprecipitation demonstrated that exposure to amlexanox was not able to induce the tyrosine phosphorylation of these receptors and was unable to prevent their tyrosine phosphorylation in response to their respective ligands (Fig. 7). In addition, ERK1 and ERK2 phosphorylation in response to either FGF1 (Fig. 6*B*) or PDGF-BB (data not shown) was not affected by exposure of quiescent Swiss 3T3 cells to amlexanox. These data suggest that the ability of polypeptide growth factors to induce the receptor tyrosine kinase activation of the mitogen-activated protein kinase pathway is independent of the presence of the F-actin cytoskeleton.

Amlexanox Inhibition of FGF1 Secretion Is Reversible—Since the effects of amlexanox on the actin cytoskeleton, cell morphology, and cell migration are reversible, we examined whether the inhibition of FGF1 release by amlexanox was also reversible. FGF1 NIH 3T3 cell transfectants were treated for 18 h with 1 mM amlexanox in the presence of 10% (v/v) BCS to produce a collapse of actin cytoskeleton. Amlexanox was removed from the medium, and the cells were subjected to heat shock (42 °C, 110 min) in the presence or absence of 0.375 mM amlexanox. As shown in Fig. 8*A*, amlexanox treatment resulted in a significant inhibition of FGF1 release, but FGF1 release was completely restored if amlexanox was removed from the cell culture medium before the temperature stress.

To further investigate the role of the actin cytoskeleton in FGF1 release, we evaluated the effect of latrunculin, a drug known to depolymerize F-actin (30), on FGF1 and p40 Syt1 release. NIH 3T3 cells stably transfected with either FGF1 (23) or with FGF1 and p65 Syt1 (4, 5) were subjected to temperature stress in the presence and absence of 400 nM latrunculin. As shown in Fig. 8, *B* and *C*, a significant inhibition of both FGF1 and p40 Syt1 release in response to heat shock was observed in the latrunculin-treated cells.

DISCUSSION

Amlexanox is a particularly efficient inhibitor of mammalian cell migration and proliferation *in vitro*. Cells exposed to amlexanox exhibited a dose-dependent inhibition of cell motility and growth without an increase in apoptotic cell death. Consistent with the inability of amlexanox to induce apoptosis, at least in concentrations used in these experiments, was the

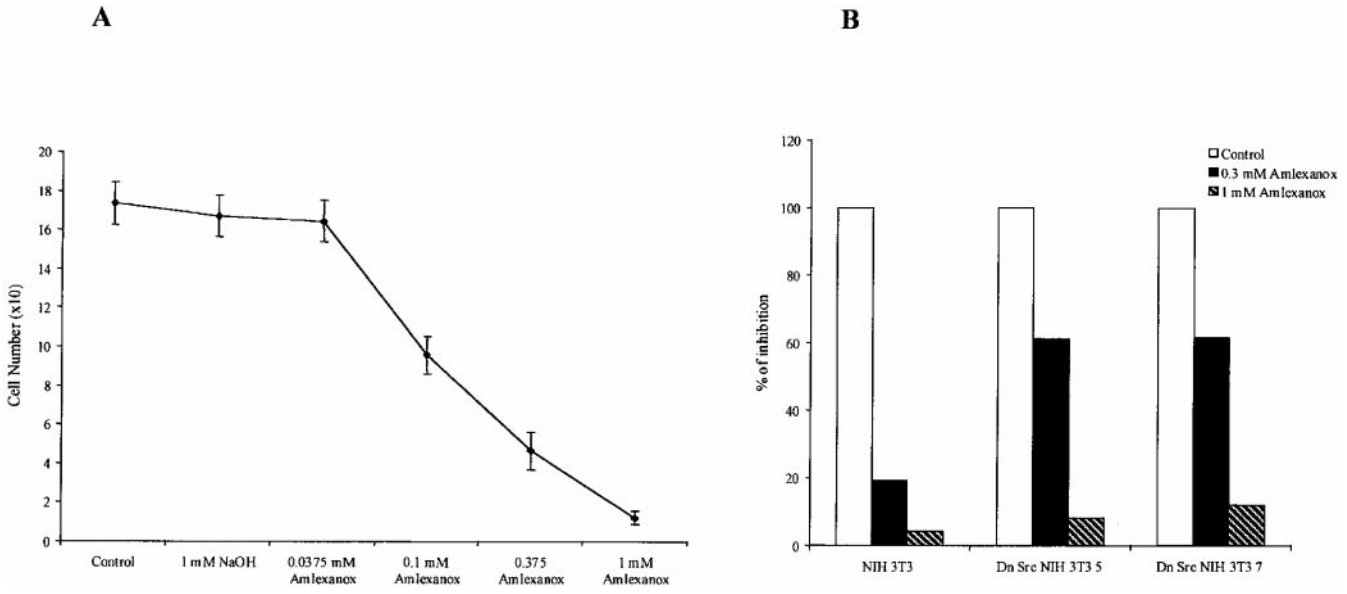

FIG. 5. **The effect of amlexanox on cell migration.** *A*, the concentration dependence of amlexanox on cell migration. NIH 3T3 cells were grown to confluence, monolayers were scraped with a razor blade, and cells were incubated for 24 h with different concentrations of amlexanox as indicated. Serum-induced cell migration into the denuded area was expressed as the number of cells present beyond the wound edge (the average of 10 microscopic fields). *B*, an assessment of the ability of amlexanox to inhibit cell migration in dnSrc NIH 3T3 cell transfectants. NIH 3T3 and dnSrc NIH 3T3 cell transfectants (clones 5 and 7) were grown to confluence, and cell migration was evaluated in the presence of 1 mM amlexanox as described previously (22). The data are reported as percent inhibition relative to the positive control.

observation that the inhibition of cell migration and proliferation by amlexanox was reversible.

In association with the suppression of cell migration and proliferation, prominent changes in cell morphology were also observed. Indeed, in most situations these morphologic changes were rapid and were readily visible after approximately 8 to 12 h. These morphologic alterations included an increase in cell size, the formation of a more flattened appearance, and the generation of long dendrite-like processes. Interestingly, the changes correlated with a strong attenuation of the presence of actin stress fibers in cells treated with amlexanox at concentrations that not only inhibit cell migration and proliferation but also alter and disorient the distribution of focal adhesion sites. In addition, we also observed more rapid and prominent morphological changes induced by amlexanox with a disappearance of actin stress fibers and subplasmalemmal cortex under serum-free conditions.

It is clear that the effects of amlexanox on the cytoskeleton are not due to the down-regulation of intracellular levels of actin or to the depolymerization of actin filaments. Also, using an *in vitro* system of actin polymerization, we observed that amlexanox was unable to inhibit this process.[2] We therefore suggest that the process of actin microfilament bundling may be involved in mediating the effects of amlexanox. Supportive of this interpretation is the observation that jasplakinolide, an agent known to stabilize actin stress fibers (20), is able to prevent the effects of amlexanox on cell morphology and actin cytoskeleton.

The mechanism utilized by amlexanox appears to involve the function of cortactin and Src. Cortactin is a Src substrate and an F-actin-binding protein whose tyrosine phosphorylation results in a dramatic reduction in F-actin cross-linking activity and actin bundling (25). Indeed, amlexanox is able to rapidly induce and sustain the tyrosine phosphorylation of cortactin, and in response to amlexanox, cortactin is able to associate with a variety of phosphotyrosine-containing proteins including a p60 polypeptide. Since it has been demonstrated that cortactin is phosphorylated by Src in response to FGF1 and other growth factors as a relatively late event in the G_1 phase of cell cycle (12, 31), we evaluated the role of Src pathway in mediating the effect of amlexanox. The overexpression of a dominant negative form of Src, known to act as an inhibitor of endogenous Src activity (18), attenuated the effect of amlexanox on both cell morphology and actin stress fibers. In addition, amlexanox was also able to significantly reduce the levels of cortactin tyrosine phosphorylation in the dnSrc NIH 3T3 cell transfectants. The dnSrc NIH 3T3 cell transfectants were also less sensitive to amlexanox-induced inhibition of cell motility and to the redistribution of focal adhesion sites, suggesting that these effects of amlexanox may also be mediated, in part, by Src.

Since it is well established that FAK is localized at focal adhesion sites (29) and is involved in the regulation of cell migration in response to extracellular stimuli (27), we evaluated whether amlexanox was able to affect FAK phosphorylation. Interestingly, amlexanox was only able to produce a moderate down-regulation of FAK phosphorylation in both NIH 3T3 and the dnSrc NIH 3T3 cell transfectants, and this effect required a prolonged exposure (3–6 h) to amlexanox. These results suggest that the redistribution of focal adhesion sites in amlexanox-treated cells may be a consequence of the collapse of the actin cytoskeleton. This interpretation is consistent with the observation that a 1-h treatment with amlexanox under conditions of serum deprivation was able to affect the intensity and the distribution of vinculin-positive focal adhesion sites in NIH 3T3 cells but not dramatically alter the tyrosine phosphorylation of FAK (data not shown).

Because the treatment of cells with amlexanox was able to prevent the FGF1-induced up-regulation of cyclin D1 in both quiescent and proliferating populations of Swiss 3T3 cells, we evaluated the capacity of FGF1, PDGF-BB, and insulin to activate their cell surface receptors in presence of amlexanox. Interestingly, the exposure of cells to amlexanox for 6 h did not prevent the ability of FGF1, PDGF-BB, and insulin to induce the auto-phosphorylation of their receptors. In addition, aml-

[2] A. Mandinova, U. Aebi, M. Landriscina, I. Prudovsky, and T. Maciag, unpublished observation.

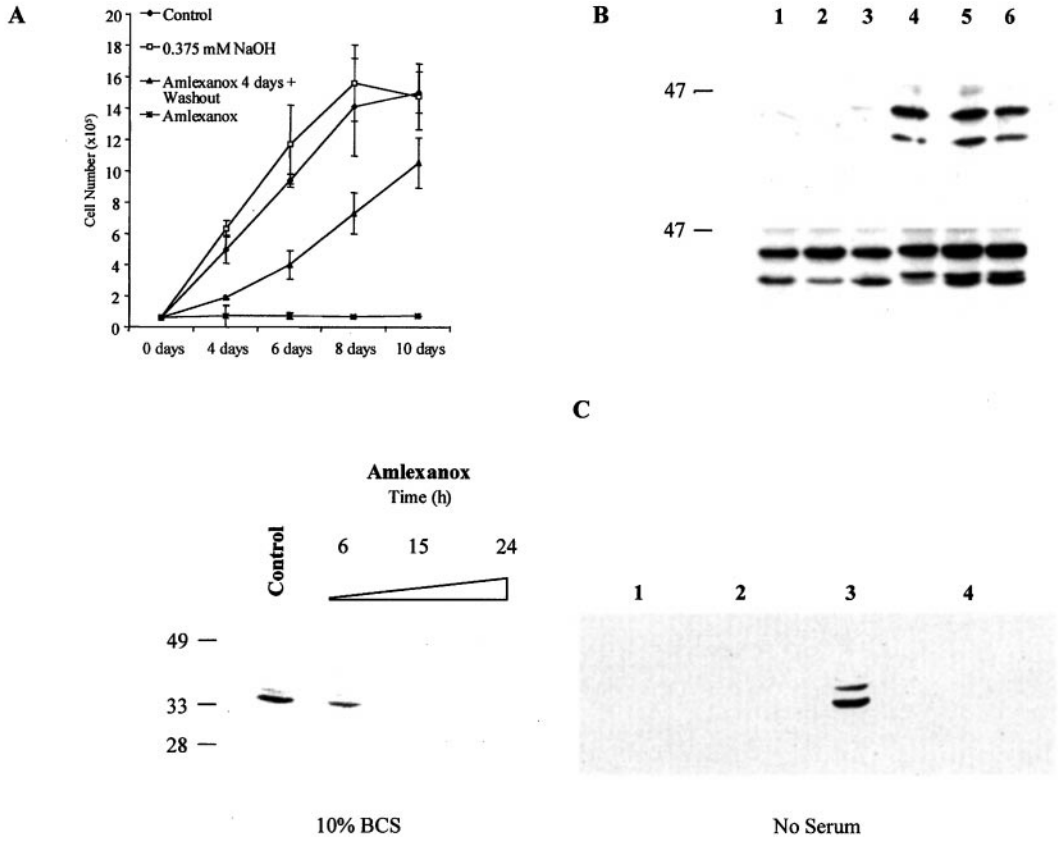

FIG. 6. **The effect of amlexanox on HUVEC proliferation and the ability of amlexanox to down-regulate cyclin D1 expression without interference with ERK1 and ERK2 tyrosine phosphorylation.** *A*, the reversibility of the inhibition of HUVEC proliferation by amlexanox; cells were grown in the presence or absence of 0.375 mM amlexanox or in the presence of 0.375 mM NaOH for 4 days, harvested by trypsin digestion, counted, and replated at a density of 6×10^4 cells/well. Cells pretreated with amlexanox were further grown in the presence or absence of the same concentration of amlexanox, and the cells pretreated with 0.375 mM NaOH were further grown in presence of 0.375 mM NaOH. Cells were harvested by trypsin digestion at 4, 6, 8, and 10 days after replating and counted in a hematocytometer. *B*, tyrosine phosphorylation of ERK1 and ERK2 in Swiss 3T3 cells treated with amlexanox. Swiss 3T3 cells were grown to confluency and incubated for 48 h in DMI. Quiescent cells were further incubated for 6 to 18 h in DMI in the presence of 1 mM amlexanox and were stimulated with 10 ng/ml FGF1 for 1 h in the presence or absence of amlexanox. Cell lysates were immunoprecipitated with polyclonal anti-ERK1 and ERK2 antibodies as described under "Materials and Methods." Immunoprecipitated proteins were resolved by 10% (w/v) SDS-PAGE and probed with an anti-phosphotyrosine antibody (*upper panel*) or with anti-ERK1 and ERK2 antibodies (*lower panel*). *Lane 1*, quiescent Swiss 3T3 cells; *lane 2*, 6 h with amlexanox; *lane 3*, 18 h with amlexanox; *lane 4*, FGF1 alone for 1 h; *lane 5*, 6 h with amlexanox and 1 h with FGF1; *lane 6*, 18 h with amlexanox and 1 h with FGF1. *C*, cyclin D1 levels in Swiss 3T3 treated with amlexanox. Quiescent Swiss 3T3 cells were stimulated for 6 h with 10 ng/ml FGF1 in either the presence or absence of 1 mM amlexanox. In a parallel experiment, Swiss 3T3 cells were grown in medium containing 10% BCS until 50% confluency and treated with 1 mM amlexanox for 6, 15, and 24 h. Cells were harvested, and cell lysates were prepared as described under "Material and Methods." Lysates were analyzed by 12% (w/v) acrylamide SDS-PAGE and probed with a mouse monoclonal anti-cyclin D1 antibody (Sigma). *Lane 1*, quiescent Swiss 3T3 cells; *lane 2*, 6 h with amlexanox; *lane 3*, 6 h with FGF1; *lane 4*, 6 h with amlexanox and FGF1.

exanox treatment did not alter the ability of FGF1 and PDGF-BB to induce ERK-1 and ERK-2 phosphorylation in quiescent Swiss 3T3 cells and did not prevent the FGF1-induced migration of ERK-1 and ERK-2 to the nucleus (data not shown). We also evaluated the capacity of amlexanox to interfere with FGFR1 activation as a function of exposure time to amlexanox using quiescent populations of Swiss 3T3 cells, and we observed a decrease in the ability of FGF1 to induce the autophosphorylation of FGFR1 only after long term exposure (18 h) of the cells to amlexanox. Shorter time periods of exposure to amlexanox, which were able to induce the disaggregation of actin cytoskeleton and prevent the up-regulation of cyclin D1, failed to interfere with receptor signaling. Since amlexanox was able to inhibit the proliferation of dnSrc NIH 3T3 cells and the induction of cyclin D1 in dnSrc NIH 3T3 cells (data not shown), we suggest that the anti-proliferative effect of amlexanox is dissociated from its effect on the Src pathway. This could be explained by the ability of amlexanox to interfere with cyclin D1 induction and the molecular events that are responsible for the G_1 transition, yet these appear to be independent of the induction of the polypeptide growth factor/receptor/Ras/mitogen-activated protein kinase signaling pathway. Our data may also suggest the importance of the actin cytoskeleton during pre-replicative events of the G_1 phase.

Other biochemical agents such as the cytochalasines and latrunculins also induce the disorganization of actin cytoskeleton as well as the inhibition of cell proliferation (30). However, unlike amlexanox, these agents induce apoptosis, and their effects on the actin cytoskeleton are more rapid and include the attenuation of stress fibers, a prominent decrease in F-actin protein levels, and a reduction in the subplasmalemmal F-actin cortex. In addition, the latrunculins and cytochalasines induce prominent cell rounding and the formation of cytoplasmic blebs, and these effects were not observed with amlexanox in the presence of serum (30). Indeed, to our knowledge, this is the first study to identify a reagent that is able to induce the reversible disassembly of actin bundles without influencing actin polymerization and inducing apoptosis. The biological activities of amlexanox may also offer novel opportunities for its use as a reagent for studies in the fields of cell biology and experimental medicine. The reversible suppression of cell growth may potentially be used to synchronize cells, and its

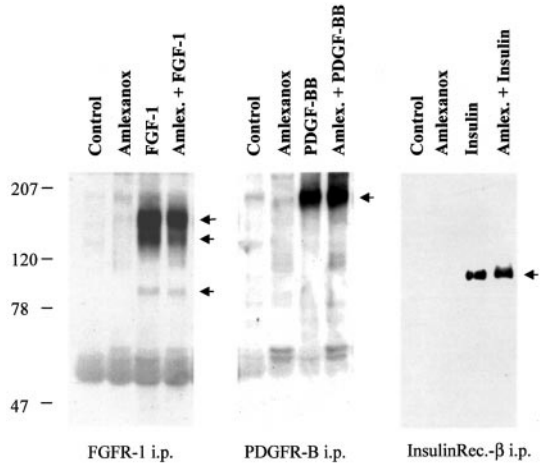

FIG. 7. **Tyrosine phosphorylation of FGFR1, PDGFR type B, and insulin receptor β subunit in Swiss 3T3 cells treated with amlexanox.** Swiss 3T3 cells were grown to confluency and then incubated in DMI for 48 h. Cells that were destined for stimulation with insulin were incubated for 48 h in insulin-free DMI. Quiescent cells were further incubated for 6 h in either serum-free medium or in the presence of 1 mM amlexanox. The cells were stimulated for 30 min with either 10 ng/ml FGF1, 5 ng/ml PDGF-BB, or 1 μg/ml insulin in the presence or absence of 1 mM amlexanox. Cell lysates were prepared and immunoprecipitated (*i.p.*) with either a polyclonal anti-FGFR1 antibody, a polyclonal anti-PDGFR type B antibody, or with a polyclonal anti-insulin receptor (*Rec.*) β subunit antibody as described under "Material and Methods." Immunoprecipitates were resolved by 7.5% (w/v) acrylamide SDS-PAGE and probed with an anti-phosphotyrosine antibody. The *arrows* indicate FGFR1α, FGFR1β, p90, PDGFR type B, and insulin receptor β subunit.

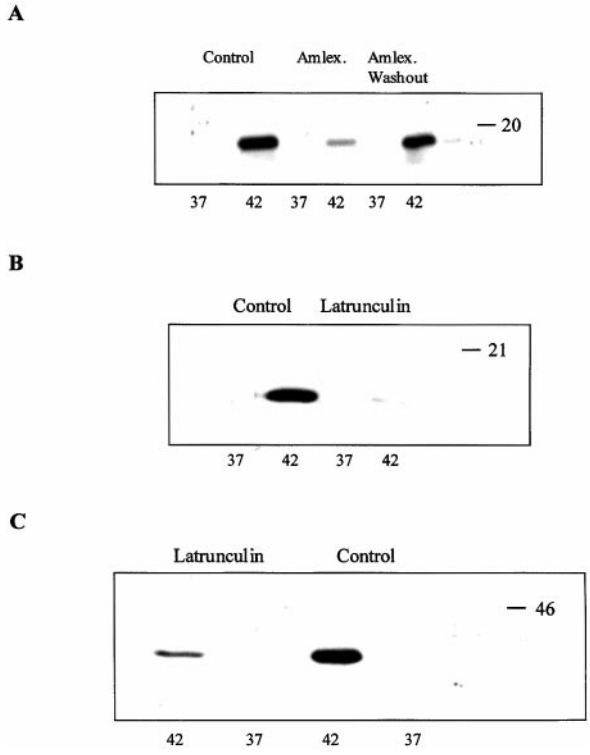

FIG. 8. **The reversible effect of amlexanox on FGF1 release and the ability of latrunculin to inhibit FGF1 and p40 Syt1 release.** *A*, NIH 3T3 cells transfected with FGF1 were grown until 70% confluence and treated for 18 h with 1 mM amlexanox to obtain a complete collapse of actin cytoskeleton. Amlexanox was removed, and the cells were incubated for 110 min at 42 °C in DMEM containing 5 units/ml heparin with and without 0.375 mM amlexanox. Conditioned media were prepared as described under "Materials and Methods," resolved by 15% (w/v) acrylamide SDS-PAGE, and subjected to immunoblot analysis with a rabbit anti-FGF1 antibody. *B* and *C*, NIH 3T3 cells transfected with FGF1 (*B*) or cotransfected with FGF1 and p65 Syt1 (*C*) were grown until 70% confluent and incubated for 110 min at 42 °C in DMEM containing 5 units/ml heparin in the presence or absence of 400 nM latrunculin. Conditioned media were prepared as described under "Materials and Methods," resolved by 12% (w/v) acrylamide SDS-PAGE, and subjected to immunoblot analysis with a rabbit anti-FGF1 (*B*) and a rabbit anti-Syt1 (*C*) antibodies.

effect on actin stress fibers may prove useful for studies of the organization and functions of the actin cytoskeleton. In addition, amlexanox may also prove useful as a reagent to assess the role of actin stress fibers in the cellular trafficking of organelles and macromolecules. Lastly, the ability of amlexanox to reversibly inhibit human endothelial cell migration and proliferation suggest that its anti-inflammatory activities *in vivo* may possess an anti-angiogenic component. However, the poor solubility of amlexanox will require the development of novel methods for the efficient *in vivo* delivery of this rather interesting biological antagonist.

The reason for studying the mechanism of amlexanox activity was the observation that amlexanox is able to bind S100A13 (14), a protein that together with Syt1 is a component of a heparin binding multiprotein complex involved in the mechanism of FGF1 release (1). Little is known about the biological functions and intracellular localization of S100A13, and it is a relatively novel member of the S100 gene family of calcium-binding proteins (32). However, it is well described that S100 gene family members, S100A1 and S100A4 (6, 7) co-localize with actin stress fibers. In addition, S100B is able to associate with the actin-capping protein, CapZ (33), and S100A2 is interactive with tropomyosins (34), which are known to regulate the bundling of actin filaments (35). Thus, the ability of amlexanox to induce cortactin tyrosine phosphorylation and to modify actin stress fibers *in vitro* may reflect either the potential co-localization of S100A13 with the actin filaments or a potential role of S100A13 to cooperate in the organization of actin cytoskeleton.

The effect of amlexanox on the Src pathway and actin stress fiber disassembly could underlie the mechanism used by this agent to interfere with the function of proteins involved in the release of FGF1 as well as its ability to suppress the release of histamine by mast cells, an important allergenic mediator (36). We observed that the effect of amlexanox on FGF1 release is reversible and correlates with the restoration of the actin cytoskeleton. Moreover, latrunculin, another reagent that affects the integrity of the actin cytoskeleton through a different mechanism that involves the depolymerization of F-actin (30), is also able to inhibit the release of FGF1 and p40 Syt1 in response to temperature stress. Thus it is possible that the function of the Src pathway and the actin cytoskeleton may be involved in the regulation of the intracellular trafficking responsible for FGF1 and Syt1 release. Since (i) p65 Syt1, a transmembrane component of intracellular vesicles (37), is involved in the regulation of exocytotic and endocytotic organelle trafficking (38), including the docking of synaptic vesicles to the plasma membrane (39), and (ii) the function of intracellular p65 Syt1 is required for FGF1 release (4), we suggest that Syt1-positive intracellular vesicles containing the extravesicular FGF1 homodimer may traffic along actin stress fibers and that the function of S100A13 or other members of the S100 gene family may be involved in the regulation of this trafficking.

Acknowledgments—We thank the officers of Takeda Pharmaceuticals, Ltd. for their generosity in supplying amlexanox, A. Mandinova and U. Aebi (University of Basel), for their assessment of the ability of amlexanox to block actin polymerization *in vitro*, and R. Friesel (Maine Medical Center) for the dnSrc mutant.

REFERENCES

1. Carreira, C., LaVallee, T., Tarantini, F., Jackson, A., Lathrop, J., Hampton, B., Burgess, W. H., and Maciag, T. (1998) *J. Biol. Chem.* **273,** 22224–22231
2. Burgess, W. H., and Maciag, T. (1989) *Annu. Rev. Biochem.* **58,** 575–606
3. Friesel, R. E., and Maciag, T. (1995) *FASEB J.* **9,** 919–925
4. LaVallee, T., Tarantini, F., Gamble, S., Carreira, C., Jackson, A., and Maciag, T. (1998) *J. Biol. Chem.* **273,** 22217–22223
5. Tarantini, F., LaVallee, T., Jackson, A., Gamble, S., Carreira, C., Garfinkel, S., Burgess, W. H., and Maciag, T. (1998) *J. Biol. Chem.* **273,** 22209–22216
6. Mandinova, A., Atar, D., Schafer, B. W., Spiess, M., Aebi, U., and Heizmann, C. W. (1998) *J. Cell Sci.* **111,** 2043–2054
7. Osterloh, D., Ivanenkov, V. V., and Gerke, V. (1998) *Cell Calcium* **24,** 137–151
8. Schmidt, A., and Hall, M. (1998) *Annu. Rev. Cell Dev. Biol.* **14,** 305–338
9. Nelson, W. J. (1991) *Semin. Cell Biol.* **2,** 375–385
10. Mulholland, J., Wesp, A., Riezman, H., and Botstein, D. (1997) *Mol. Biol. Cell* **8,** 1481–1499
11. Felsenfeld, D., Schwartzberg, P., Venegas, A., Tse, R., and Sheetz, M. (1999) *Nat. Cell Biol.* **1,** 200–206
12. Zhan, X., Hu, X., Hampton, B., Burgess, W. H., Friesel, R., and Maciag, T. (1993) *J. Biol. Chem.* **268,** 24427–24431
13. LaVallee, T. M., Prudovsky, I. A., McMahon, G. A., Hu, X., and Maciag, T. (1998) *J. Cell Biol.* **141,** 1647–1658
14. Oyama, Y., Shishibori, T., Yamashita, K., Naya, T., Nakagiri, S., Maeta, H., and Kobayashi, R. (1997) *Biochem. Biophys. Res. Commun.* **240,** 341–347
15. Maciag, T., Cerundolo, J., Ilsley, S., Kelley, P. R., and Forand, R. (1979) *Proc. Natl. Acad. Sci. U. S. A.* **76,** 5674–5678
16. Winkles, J. A., Alberts, G. F., Peifley, K. A., Nomoto, K., Liau, G., and Majesky, M. W. (1996) *Am. J. Pathol.* **149,** 2119–2131
17. Libermann, T. A., Friesel, R., Jaye, M., Lyall, R. M., Westermark, B., Drohan, W., Schmidt, A., Maciag, T., and Schlessinger, J. (1987) *EMBO J.* **6,** 1627–1632
18. Thomas, J., Soriano, P., and Brugge, J. S. (1991) *Science* **254,** 568–571
19. Zhan, X., Hu, X., Friesel, R., and Maciag, T. (1993) *J. Biol. Chem.* **268,** 9611–9620
20. Cramer, L. (1999) *Curr. Biol.* **9,** 1095–1105
21. Chan, A. Y., Raft, S., Bailly, M., Wyckoff, J., Segall, J., and Condeelis, J. S. (1998) *J. Cell Sci.* **111,** 199–211
22. Sato, Y., and Rifkin, D. B. (1988) *J. Cell Biol.* **107,** 1199–1205
23. Jackson, A., Friedman, S., Zhan, X., Engleka, K. A., Forough, R., and Maciag, T. (1992) *Proc. Natl. Acad. Sci. U. S. A.* **89,** 10691–10695
24. Garfinkel, S., Hu, X., Prudovsky, I. A., McMahon, G. A., Kapnik, E. M., McDowell, S. D., and Maciag, T. (1996) *J. Cell Biol.* **134,** 783–791
25. Huang, C., Ni, Y., Wang, T., Gao, Y., Haudenschild, C. C., and Zhan, X. (1997) *J. Biol. Chem.* **272,** 13911–13915
26. Pavalko, F., Otey, C., Simon, K., and Burridge, K. (1991) *Biochem. Soc. Trans.* **19,** 1065–1069
27. Sheetz, M., Felsenfeld, D., and Galbraith, C. (1998) *Trends Cell Biol.* **8,** 51–54
28. Craig, S., and Johnson, R. (1996) *Curr. Opin. Cell Biol.* **8,** 74–85
29. Schaller, M., Hildebrand, J., and Parsons, J. (1999) *Mol. Biol. Cell* **10,** 3489–3505
30. Spector, I., Shochet, N. R., Blasberger, D., and Kashman, Y. (1989) *Cell Motil. Cytoskeleton* **13,** 127–144
31. Zhan, X., Plourde, C., Hu, X., Friesel, R., and Maciag, T. (1994) *J. Biol. Chem.* **269,** 20221–20224
32. Wicki, R., Schafer, B. W., Erne, P., and Heizmann, C. W. (1996) *Biochem. Biophys. Res. Commun.* **227,** 594–599
33. Kilby, P. M., Van Eldik, L. J., and Roberts, G. C. (1997) *Protein Sci.* **6,** 2494–2503
34. Gimona, M., Lando, Z., Dolginov, Y., Vandekerckhove, J., Kobayashi, R., Sobieszek, A., and Helfman, D. M. (1997) *J. Cell Sci.* **110,** 611–621
35. Ishikawa, R., Yamashiro, S., Kohoma, K., and Matsumura, F. (1998) *J. Biol. Chem.* **273,** 26991–26997
36. Makino, H., Saijo, T., Ashida, H., Kuriki, H., and Maki, Y. (1987) *Int. Arch. Allergy Appl. Immunol.* **82,** 66–71
37. Perin, M. S., Brose, N., Jahn, R., and Sudhof, T. C. (1991) *J. Biol. Chem.* **266,** 623–629
38. Zhang, J. Z., Davletov, B. A., Sudhof, T. C., and Anderson, R. G. W. (1994) *Cell* **78,** 751–760
39. Sollner, T., Whiteheart, S. W., Brunner, M., Erdjument-Bromage, H., Geromanos, S., Tempst, P., and Rothman, J. (1993) *Nature* **362,** 318–324